ChemComm

Accepted Manuscript

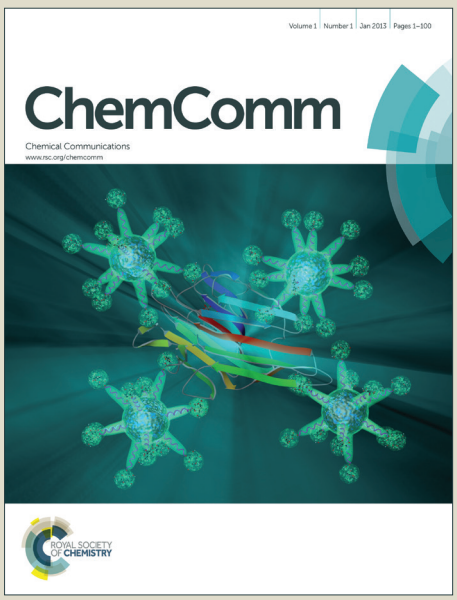

ROYAL SOCIETY OF CHEMISTRY

www.rsc.org/chemcomm

Journal Name

COMMUNICATION

Design isolated iron species for Fenton reaction: lyophilization beat calcination treatment

Received 00th January 20xx,
Accepted 00th January 20xx

DOI: 10.1039/x0xx00000x

www.rsc.org/

Leitao Zhang, Hui Ye, Lizhi Zhao, Lei Zhang, Lili Yao, Yuzhong Zhang,* and Hong Li

Lyophilization is used to prepare Fenton catalyst containing predominant amount of isolated Fe^{3+} species with 8.90 % iron content, which shows higher catalytic rate and H_2O_2 utilization efficiency but lower iron leaching in phenol degradation, compared with the calcination sample.

Bio-recalcitrant wastewater has become a pervasive problem afflicting people throughout the world due to negative impacts for ecosystems and humans.[1,2] Among abatement technologies for wastewater, Fenton system is the most attractive method because of its fast reaction rate, low toxicity, and simplicity to control.[3] Nevertheless, a main drawback of Fenton reaction is the need of stoichiometric amounts of iron salts.[4] To conquer the drawback, various solid matrixes[5-9] have been developed as heterogeneous Fenton catalysts supports in recent decades. Zeolites are widely used in catalysis due to their uniform, small pore size, large internal surface area, flexible frameworks, and controlled chemistry.[10] However, these iron oxide-containing zeolite materials suffer from iron agglomeration and leaching (from 6 to 100wt %) in Fenton-like reaction.[11] Additionally, H_2O_2 is an expensive commodity,[12] and its excess must be greatly reduced. But little attention is paid to the utilization efficiency of H_2O_2 in Fenton reaction.

It is established that the tetrahedrally coordinated and atomically isolated $[MO_4]$ (M=Fe, Co, etc.) species play a favourable role in zeolite catalysis.[13-18] Ye et al.[15] and Timofeeva et al.[11] reported that atomically isolated Fe^{3+} sites exhibited higher catalytic activity than small iron oxide clusters and particles and were responsible for the iron anti-leaching during the catalytic reactions. Wang et al.[16] pointed that the catalyst with predominant isolated Cu^{2+} sites manifested the most excellent catalytic activity and highest H_2O_2 efficiency in phenol hydroxylation process, whereas the one containing the most copper oxide clusters showed the lowest rate and utilization efficiency of H_2O_2. In addition, zeolites containing isolated tetrahedral $[MnO_4]$[17] and $[CoO_4]$[18] species were active in selective catalytic oxidation or reduction. However, it was found that only with low metal content (<2 wt. %) in these catalysts, the majority of total metal species were present in form of isolated $[MO_4]$ (M=Fe, Co, etc.) sites.[11,19]

Freeze-drying is a drying method often encountered in food processing as well as in the pharmaceutical industry usually for preservation purposes.[20] Although there have been some literatures on the application of freeze drying in catalyst preparation, the aim of lyophilization is to pretreat the catalyst precursors and to control the nanoparticle distribution uniformity.[20,21] In this work, to the best of our knowledge, lyophilization is first used to prepare Fenton catalyst containing predominant amount of isolated Fe^{3+} species with 8.90 wt. % iron content, which is the maximum metal content in catalysts containing predominant amount of isolated metal sites so far. Compared with the calcination sample, the lyophilization catalyst shows higher catalytic rate and H_2O_2 utilization efficiency but lower iron leaching in phenol degradation.

Scheme 1 illustrates the preparation process. Catalyst precursor with 8.90% iron content is firstly obtained through the blend of 10 g 4A zeolite and 500ml 2000mg/L $FeCl_3$ solution. Then the catalyst

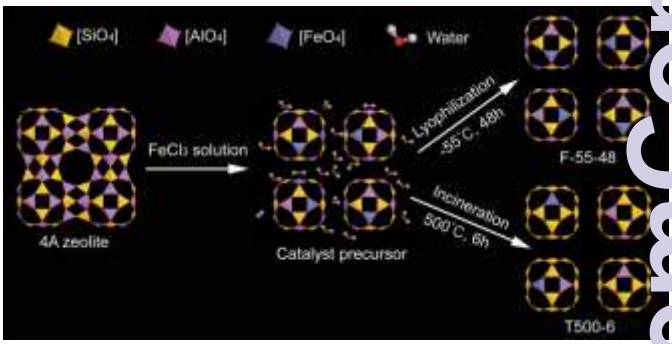

Scheme 1 Synthesis of F-55-48 and T500-6 catalysts and the suppositional existence state of tetrahedral $[TO_4]$ (Fe, Al and Si) sites.

State Key Laboratory of Separation Membranes and Membrane Processes, School of Materials Science and Engineering, Tianjin Polytechnic University, Tianjin, 300387 (P.R. China).
E-mail: zhangyz2004cn@vip.163.com

† Footnotes relating to the title and/or authors should appear here.
Electronic Supplementary Information (ESI) available: [details of any supplementary information available should be included here]. See DOI: 10.1039/x0xx00000x

precursor is lyophilized at -55°C for 48h and labelled as F-55-48. By contrast, T500-6 is obtained through catalyst precursor calcination at 500°C for 6h (Experimental details are available in ESI†). XPS characterizations (Fig. S6, ESI†) provide detailed information about the oxidation state of iron element, suggesting that only Fe^{3+} exists in all catalysts. Compared with neat surface of 4A zeolite (Fig. S4, ESI†), the SEM images show the surface of the catalysts becomes rough with iron loading on the zeolite (Fig. 1a, b). The TEM images (Fig. 1c, d and Fig. S5a, b, c, ESI†) exhibit few iron oxide aggregates in F-55-48 material but large amount of aggregates in T500-6 one (Fig. 1e and Fig. S5d, e, ESI†). These iron aggregates display a lattice spacing of 0.368nm (Fig. 1f), corresponding to the (012) plane, and are attributed as α-Fe_2O_3, in good parallel with the XRD analysis (Fig. S3, ESI†).

UV/Vis spectrum is extensively employed to characterize the nature and coordination environment of iron species in iron-containing silicate materials (Fig. 2). The comparison of the 4A zeolite and iron-containing catalysts indicates that the enhanced adsorption in catalysts arises from the presence of iron species. The spectra can be divided into three parts: wavelengths at 200<λ<300 nm, 300<λ<400 nm and >400 nm.[19] According to the Tanabe and Sugano diagram,[22] the two bands observed at ca. 209 nm and 276 nm are attributed to the $t_1 \rightarrow t_2$ and $t_1 \rightarrow e$ transitions involving Fe^{3+} in the [FeO_4] tetrahedral group, respectively. The bands at 300<λ<400 nm are assigned to small oligomeric Fe_xO_y clusters inside pores and bands >400 nm are assigned to large Fe_2O_3 particles.[19] According to

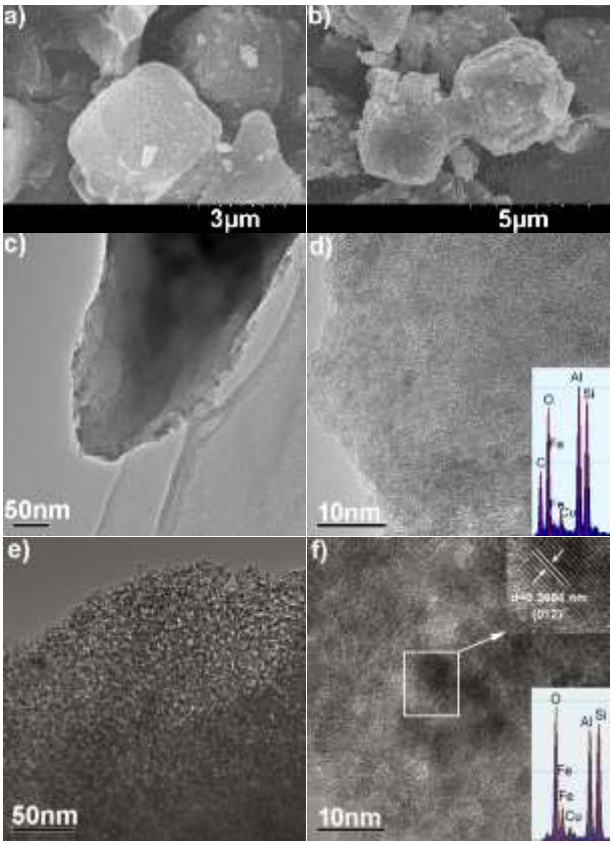

Fig. 1 SEM images of a) F-55-48, and b) T500-6. TEM images of c, d) F-55-48 (inset: EDS element analysis) and e, f) T500-6 (inset: exploded view (top) and EDS element analysis).

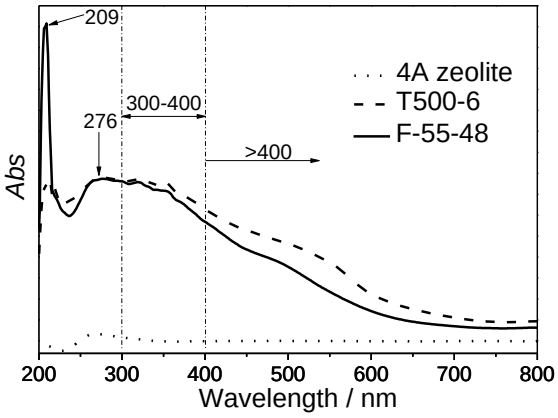

Fig. 2 UV/Vis spectra of 4A zeolite, T500-6 and F-55-48 catalyst.

the Kubelka-Munk representation,[23] it can be calculated roughly that about 85.87% Fe sites are isolated iron species in lyophilized catalyst but only 41.57% isolated iron sites remain in contrastive sample. In addition, the transverse vibrations (Eu) at 450 cm attributed to the Fe-O-Fe stretching mode[24] appears in T500-6 but not in F-55-48 material (Fig. S10a, ESI†). All these data, combined with the TEM images analysis, suggest that predominant amount of iron species in F-55-48 are isolated iron sites but those in T500-6 catalyst are iron oxide aggregates. The EPR spectra provide further evidence for predominated amount of isolated iron sites in F-55-48 catalyst and iron oxides in T500-6 sample (detailed analysis in S3.4 part, ESI†). Additionally, the comparison of the metal content (<20 wt. %) with other literatures[11,14,15,17,19,20] suggests that this is the maximum metal content (8.90 wt. %) in catalysts containing predominant amount of isolated metal sites so far.

The IR spectra (Fig. S10a, ESI†) confirm the external linkages of 4A zeolite are destroyed, but the internal [TO_4] (T=Si, Al) tetrahedral primary units are still reserved. The XPS spectra (Fig. S10b, ESI†) demonstrate that 74.73% [AlO_4] primary building units still exist in F-55-48 sample but only 5.24% is remained in T500-6 catalyst (Table 1). Scheme 1 shows the suppositional existence state of [TO_4] (T=Fe, Al and Si elements) units in different materials (detailed analysis in S3.6, ESI†). The N_2 adsorption-desorption isotherms infer that the specific surface area of the as-prepared material with lyophilization is 126.01$m^2 g^{-1}$, which is far larger than T500-6 sample (9.04 $m^2 g^{-1}$). There appear mesopores (4.31 nm) in the F-55-48 catalyst whereas the mean-pore size of T500-6 is only 1.39 nm (Table 1).

Concerning the reason of the tremendous differences between F-55-48 and T500-6 material, the two steps in catalyst preparation

Table 1 Physical properties of 4A zeolite, F-55-48 and T500-6.

Samples	Surface area[a] ($m^2 g^{-1}$)	Pore size (nm)	[AlO_4]/total Al[d] (At. %/At. %)
4A zeolite	573.00	0.41	100.00%
F-55-48	126.01	4.31[b]	74.73%
T500-6	9.04	1.39[c]	5.24%

[a] Obtained by BET measurement. [b] Calculated by BJH method. [c] Calculated by DFT analysis. [d] Obtained by XPS analysis (See detailed analysis in S3.4 part, ESI†).

process need to be analysed. Firstly, the crystalline structure of 4A zeolite disappears after mixing with $FeCl_3$ solution (Fig.S2, ESI†) because of the acid leaching[25] and the exchange of Al^{3+} and Fe^{3+} (detailed analysis in S5, ESI†). The acid leaching creates mesopores[10] and the ion exchange leads to [FeO_4] tetrahedrons[26] in the precursor. Secondly, the lyophilization process only sublimates the "ice template"[27] insides pores and holds the mesoporous structure, whereas high temperature forces not only the water out of the pores but also framework iron and aluminium species into extraframework clustered iron or aluminium oxides. The migration leads to the decrease in the amount of tetrahedral [FeO_4] and [AlO_4] units in catalysts. And these forming clustered oxides species obstruct the channels and result in the decrease of the specific surface area and pore size of T500-6 catalyst.

The catalytic performance of as-prepared materials is evaluated for the phenol degradation (Fig. 3). The adsorption study indicates that there is no phenol adsorption on catalysts (Fig. S23, ESI†). In Fig.3a, for F-55-48 catalyst, with initial pH=2.00, nearly 97.15% of the phenol is degraded within 13.5 min, whereas 110 min is needed for T500-6 to achieve the same degradation efficiency. This results from the difference of induction period[16] which is the unique feature of radical-type mechanism confirmed by *tert*-butanol and DMSO[28] quenching experiments (Fig. S14, ESI†). The induction period is an activation process of iron species[29] and shorter induction time infers higher catalytic activity of F-55-48 catalyst (detailed mechanism in S6.3, ESI†). Phenol degradation under different pH conditions verifies again the high catalytic activity of F-55-48 catalyst (Fig. S15, ESI†). We further confirm the effectiveness of lyophilization in catalyst preparation by the comparison of other freeze-dried and calcination catalysts (Fig. S18a, ESI†).

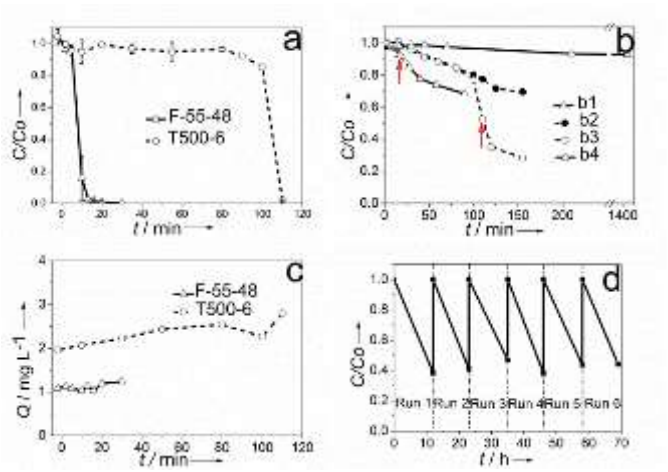

Fig. 3 (a) Phenol degradation in the presence of F-55-48 and T500-6 catalysts. (b) The influence of the absence or presence of phenol on H_2O_2 degradation with different catalysts: b1) no phenol, F-55-48; b2) no phenol, T500-6; b3) phenol, T500-6; b4) phenol, F-55-48. Red arrow indicates the time of phenol complete degradation. (c) Iron leaching in phenol degradation with different catalysts. (d) Successive recycling experiment of F-55-48 for phenol degradation at initial pH=6.30. Other conditions: Phenol=200 mg/L, 100 mL; H_2O_2/Phenol=12.75 (molar ratio); Catalyst=0.10 g; Initial pH=2.00±0.01; T=25 °C

During phenol degradation, the concentration of H_2O_2 is detected to study the H_2O_2 utilization efficiency. Fig.3b shows the change of residual H_2O_2 concentration in phenol degradation with different catalysts. In the presence of phenol, after phenol complete degradation, one can observe that residual H_2O_2 concentration is higher with F-55-48 than the one with T500-6 (Fig.3b, b3 and b4). This infers that F-55- 48 shows higher H_2O_2 utilization efficiency than T500-6. To shed light on this reason, we perform twin experiments in which the degradation of H_2O_2 in the absence of phenol by F-55-48 and T500-6 (Fig.3b, b1 and b2). The twin experiments uncover T500-6 catalyst containing large amount of iron oxide aggregates disproportionates hydrogen peroxide into non-productive oxygen molecular, which leads to the low H_2O_2 efficiency. The other results indicate that all lyophilization catalysts exhibit higher H_2O_2 efficiency than calcination samples as outlined in Table S3.

The stability of freeze-dried catalysts is evaluated by the measurement of iron leaching and successive recycling experiment. Fig. 3c shows the average iron leaching of F-55-48 catalyst is around 1.14mg L^{-1} in phenol degradation process, whilst the value of T500-6 catalyst is 2.37mg L^{-1}. Similarly, the other lyophilization catalysts exhibit lower iron leaching in catalytic process (Fig. S18b and Table S1, ESI†). This means that the freeze-dried samples may have better stability than calcination catalysts. Six successive recycling experiments are carried out at initial pH=6.30 (Fig.3d) and the experiment results and the characterizations of used catalyst (detailed information in S8, ESI†) further show good stability of F-55-48 catalyst. However, T500-6 catalyst appears poorer stability for phenol degradation in three successive tests (S10, ESI†).

As mentioned before, the freeze-dried catalysts have predominant amount of isolated Fe^{3+} species with 8.90% iron content and the isolated Fe^{3+} sites have highly catalytic performance, so it can be supposed that the presence of predominant amount of isolated iron species is the dominant reason why lyophilization catalysts display superior catalytic performance than calcination ones. Besides, the generation of mesopores[30] and larger specific surface area, and more tetrahedral [AlO_4] sites[31,32] in lyophilization materials may be beneficial to its enhanced catalytic activity. Besides, the fact that catalysts prepared at room temperature show weak catalytic performance for phenol degradation due to their poor dispersion in reaction medium further manifests the advantages of lyophilization in catalyst preparation (more information in S7, ESI†).

In conclusion, lyophilization is used to prepare Fenton catalysts containing predominant amount of isolated Fe^{3+} species with 8.90 wt. % iron content, which is the maximum metal content in catalysts containing predominant amount of isolated metal sites so far. Compared with calcination catalysts, the as-prepared samples exhibit higher catalytic degradation rate and H_2O_2 efficiency for phenol but lower iron leaching in catalytic reaction. The lyophilization method only removes the water in catalyst precursor and reserves predominant amount of isolated iron sites which play a key role in enhancing catalytic performance. Nevertheless, the migration of isolated iron/aluminum sites caused by calcination from framework positions to extraframework clusters or particles leads to disadvantages. This study identifies a promising new

strategy for engineering practical catalysts for environment remediation.

This work is supported by the National Natural Science Foundation of China (No. 51503146, 51173132, 51373120, and 21204064), Science and Technology Commission Foundation of Tianjin (No.15JCZDJC37600, and 14JCQNJC03900), Public Science and Technology Research Funds Projects of Ocean (201305004-5), and Research Fund for the Doctoral Program of Higher Education (Funding No.20111201110003).

Notes and references

1 M. A. Shannon, P. W. Bohn, M. Elimelech, J. G. Georgiadis, B. J. Marinas and A. M. Mayes, *Nature*, 2008, **452**, 301.
2 A. Turki, C. Guillard, F. Dappozze, Z. Ksibi, G. Berhault and H. Kochkar, *Appl. Catal., B*, 2015, **163**, 404.
3 N. A. Zubir, C. Yacou, J. Motuzas, X. Zhang, X. S. Zhao and J. C. Diniz da Costa, *Chem. Commun.*, 2015, **51**, 9291.
4 S. Navalon, M. Alvaro and H. Garcia, *Appl. Catal., B*, 2010, **99**, 1.
5 S. Navalon, A. Dhakshinamoorthy, M. Alvaro and H. Garcia, *ChemSusChem*, 2011, **4**, 1712.
6 J. Herney-Ramirez, M. A. Vicente and L. M. Madeira, *Appl. Catal., B*, 2010, **98**, 10.
7 A. Dhakshinamoorthy, S. Navalon, M. Alvaro and H. Garcia, *ChemSusChem*, 2012, **5**, 46.
8 H. Lim, J. Lee, S. Jin, J. Kim, J. Yoon and T. Hyeon, *Chem. Commun.*, 2006, DOI: 10.1039/B513517F, 463.
9 H. Sun, Y. Wang, S. Liu, L. Ge, L. Wang, Z. Zhu and S. Wang, *Chem. Commun.*, 2013, **49**, 9914.
10 Y. Tao, H. Kanoh, L. Abrams and K. Kaneko, *Chem. Rev.*, 2006, **106**, 896.
11 M. N. Timofeeva, M. S. Melgunov, O. A. Kholdeeva, M. E. Malyshev, A. N. Shmakov and V. B. Fenelonov, *Appl. Catal., B*, 2007, **75**, 290.
12 S. Navalon, R. Martin, M. Alvaro and H. Garcia, *Angew. Chem.*, 2010, **122**, 8581.
13 Y. Sun, S. Gao, F. Lei and Y. Xie, *Chem. Soc. Rev.*, 2015, **44**, 623.
14 S. Yashnik and Z. Ismagilov, *Appl. Catal., B*, 2015, **170–171**, 241.
15 Y. Wang, Q. Zhang, T. Shishido and K. Takehira, *J. Catal.*, 2002, **209**, 186.
16 G. Zhang, J. Long, X. Wang, Z. Zhang, W. Dai, P. Liu, Z. Li, L. Wu and X. Fu, *Langmuir*, 2009, **26**, 1362.
17 Y. Meng, H. C. Genuino, C.-H. Kuo, H. Huang, S.-Y. Chen, L. Zhang, A. Rossi and S. L. Suib, *J. Am. Chem. Soc.*, 2013, **135**, 8594.
18 J. Janas, T. Machej, J. Gurgul, R. P. Socha, M. Che and S. Dzwigaj, *Appl. Catal., B*, 2007, **75**, 239.
19 M. Santhosh Kumar, M. Schwidder, W. Grünert, U. Bentrup and A. Brückner, *J. Catal.*, 2006, **239**, 173.
20 T. M. Eggenhuisen, P. Munnik, H. Talsma, P. E. de Jongh and K. P. de Jong, *J. Catal.*, 2013, **297**, 306.
21 G. Chen and W. Wang, *Drying Technol.*, 2007, **25**, 29.
22 S. Bordiga, R. Buzzoni, F. Geobaldo, C. Lamberti, E. Giamello, A. Zecchina, G. Leofanti, G. Petrini, G. Tozzola and G. Vlaic, *J. Catal.*, 1996, **158**, 486.
23 P. Boroń, L. Chmielarz and S. Dzwigaj, *Appl. Catal., B*, 2015, **168**, 377.
24 R. M. Cornell and U. Schwertmann, The iron oxides: structure, properties, reactions, occurrences and uses, John Wiley & Sons, 2006.
25 A. H. Janssen, A. J. Koster and K. P. de Jong, *Angew. Chem., Int. Ed.*, 2001, **40**, 1102.
26 E. Díaz, S. Ordóñez, A. Vega and J. Coca, *Appl. Catal., B*, 20[illegible], **56**, 313.
27 W. Chen, Y.-X. Huang, D.-B. Li, H.-Q. Yu and L. Yan, *RSC Adv*[illegible] 2014, **4**, 21619.
28 S. Enami, Y. Sakamoto and A. J. Colussi, *PNAS*, 2014, [illegible], 623.
29 L. Xu and J. Wang, *J. Hazard. Mater.*, 2011, **186**, 256.
30 S. Van Donk, A. H. Janssen, J. H. Bitter and K. P. de Jon[illegible], *Catal. Rev.*, 2003, **45**, 297.
31 N. Musselwhite, K. Na, S. Alayoglu and G. A. Somorjai, *J. Am*[illegible] *Chem. Soc.*, 2014, **136**, 16661.
32 A. L. T. Pham, C. Lee, F. M. Doyle and D. L. Sedlak, *Environ. Sci. Technol.*, 2009, **43**, 8930.